

## FATIGUE FRACTURE IN A RUBBER-TOUGHENED GLASSY POLYMER

M. Rink\*, D. Imbrighi\*, L. Castellani\*\*, A. Pavan\*

The fatigue behaviour of a series of rubber-modified glassy polymers made of a styrene-acrylonitrile copolymer modified with different amounts of an olefin rubber was investigated. Tests were performed on sharply notched samples, and both stages of fatigue lifetime, i.e. crack initiation and crack propagation, were examined. The most interesting result appears to be that, for a given applied stress intensity factor range, at least under the conditions adopted in this work, fatigue lifetime increases with rubber content up to a certain content, after which a decrease in lifetime is observed.

### INTRODUCTION

It has often been recalled (1,2,3,4) that the effect of the rubber modification of glassy polymers on fatigue fracture is not always straightforward. Furthermore, material optimization for fatigue fracture is not necessarily in agreement with that for other fracture properties; caution must thus be used to ensure adequate fatigue performance for these materials. Different effects of rubber modification on the two stages of fatigue failure (crack initiation and crack propagation) have been suggested on the grounds of the inconsistent results obtained in tests on unnotched specimens, where the initiation stage is predominant, as compared with those obtained on notched specimens. In this paper we present some results on fatigue failure in notched specimens of a series of rubber-modified materials with varying dispersed-phase content. Both stages of fatigue failure have been considered, and the influence of rubber content on fatigue lifetime has been analyzed.

\*Dip. Chim. Ind. e Ing. Chim., Politecnico di Milano (Italy).

\*\*Montedipe, Mantova (Italy).

MATERIALS

An olefin rubber modified styrene acrylonitrile copolymer (AES), produced by Montedipe through a continuous bulk polymerization process, was used for this work. Base material, AES-40, consists of a continuous styrene-acrylonitrile (SAN) phase, in which approximately spherical rubber-phase particles are dispersed. The characteristics of the experimental samples are shown in Table 1. Samples AES-5 to AES-25, with different amounts of rubber-phase, were prepared by extrusion-blending the base material with suitable amounts of a SAN copolymer (named AES-0), whose molecular weight distribution was chosen to match that of the matrix of the base sample. A commercial grade sample, AES-B27, having different SAN molecular weight distribution (MWD) and different dispersed particle size distribution from the AES-5 - AES-40 series materials, was also investigated.

TABLE 1 - Characteristics of samples examined ( $M_w$  and  $M_n$  = weight average and number average molecular weights respectively).

SAMPLE	RUBBER CONTENT (Weigth %)	SAN MATRIX	
		( $M_w$ )	( $M_w/M_n$ )
AES-0	0	95600	1.726
AES-5	5.8	92700	1.748
AES-15	15	92800	1.757
AES-25	24.1	89140	1.745
AES-40	39.4	91520	1.735
AES-B27	27.3	84500	1.700

EXPERIMENTAL DETAILS

All test samples were of single edge-notch (SEN) geometry with dimensions of 104 x 23 x 3 mm. Sharp notches (tip radius about 10  $\mu$ m) were made with a flying cutter. Tests were performed, at 23°C, in tension, with bending restrained, on an Instron servo-hydraulic machine, under both load and displacement control. Fracture mechanics was applied: stress intensity factors were calculated using a calibration factor experimentally determined for the

geometry adopted:

$$K = \frac{P}{WB} Y(a/W) \sqrt{a} \quad Y(a/W) = \left[ \frac{0.74}{\pi} \cdot 10 \left( 0.66 + 0.74 (a/W)^2 \right) \right]^{1/2}$$

in which P is the applied load, W and B are specimen width and thickness respectively, and a is the crack length.

Crack growth was monitored by means of a videorecording system. Both stages, crack initiation (FCI) and crack propagation (FCP), were considered: the number of cycles to initiate crack propagation and fatigue lifetime were related to the applied stress intensity factor range,  $\Delta K$ , and plots of crack growth rate,  $da/dN$ , vs.  $\Delta K$  were made to characterize FCP when continuous crack growth was observed.

On sample AES-B27, preliminary tests at 1 Hz, varying notch length, stress and displacement amplitude, and maximum to minimum stress ratio, R, were performed. From these it appeared that  $\Delta K$  seems to be the parameter controlling FCI and FCP under both load and displacement control. On this sample some tests were also carried out at 10 Hz, to check frequency sensitivity. On samples AES 0 - AES 40, tests were conducted at 1 Hz and a range of applied  $\Delta K$ .

### RESULTS AND DISCUSSION

Sample AES-B27 - Fatigue tests at 1 Hz (11 in load control and 19 in displacement control) and at 10 Hz (2 in load control and 3 in displacement control) on sample AES-B27 all showed continuous crack propagation. Figures 1a and 1b report plots of the applied  $\Delta K$  as a function of the number of cycles to initiate crack propagation and the number of cycles for propagation, respectively. Figure 2 shows FCP behaviour for the same tests (lines are averages of all the tests performed). It is to be noticed that:

- i) Although notched samples were adopted a large part of fatigue lifetime is due to crack initiation.
- ii) While crack initiation does not seem to be influenced by the control mode (Figure 1a), the propagation stage shows a clear difference between the two modes (Figure 1b).
- iii) A positive frequency sensitivity factor (fsf) is observed both in load and displacement control: FCP decreases upon increasing frequency from 1 to 10 Hz (Figure 2).

From these results it may be thought that in sample AES-B27 only localized heating takes place. In fact, previously (1,3) positive frequency sensitivity factors have been ascribed to localized hysteretic heating at the crack tip, while negative fsf have been related to a generalized heating of the sample. The independence of FCI from the control mode can be related to the fact that during this phase of fatigue lifetime hysteretic heating at the crack tip, which

depends (5) on  $\Delta K^2$ , is similar for both control modes. When the crack begins to propagate, hysteretic heating proceeds differently: the rate of temperature increase with crack length,  $dT/da$ , is related (5) to the K-gradient,  $dK/da$ , which is dependent on the control mode.

*Samples AES-0 - AES-40* - Fatigue tests on the series of materials with varying rubber content (AES-0 - AES-40) showed discontinuous FCP. Thus  $da/dN$  vs.  $\Delta K$  plots had no significance and only diagrams of applied  $\Delta K$  vs. cycles to initiate fracture and cycles to failure are reported (Figures 3a and 3b respectively). From these it can be observed that:

- i) Time to failure is practically entirely due to the initiation process for the neat SAN resin and for the two AES samples with 5% and 15% dispersed phase; for the samples with rubber contents of 25% and 40%, FCI still covers a substantial portion of fatigue lifetime.
- ii) Regarding the effect of dispersed phase content, it appears that fatigue lifetime is maximum for a certain rubber amount; in fact, for a given applied stress intensity factor range,  $\Delta K$ , fatigue lifetime increases with rubber content up to a certain content (25% for the series examined), after which a decrease in lifetime is observed. This behaviour can again be thought of as an effect of different hysteretic heating (6): rubber toughened materials generally have a higher level of viscoelastic damping, and thus higher hysteretic heating, compared with that of the unmodified matrix. In notched samples up to a certain rubber content, heating is probably only localized, as results in sample AES-B27 seem to show, and this effect appears beneficial, as already observed by other authors (5); when rubber content exceeds a certain level, heating may become more generalized and crack propagation may be enhanced (5).

A final observation on these results comes from comparison between the behaviour of samples AES-B27 and AES-25. These two samples, which have practically the same rubber content, differ in molecular weight, molecular weight distribution, and dispersed particle size distribution. Although their total fatigue lifetime did not differ substantially, sample AES-B27 showed continuous FCP, while sample AES-25 displayed discontinuous FCP. This different crack propagation mode could be due to the different MWD between the two samples, since it has previously been shown that the existence of discontinuous growth bands appears to depend strongly on molecular weight and MWD (2,6)

REFERENCES

- (1) J. A. Manson et al.; Toughening of Plastics II, Plastics and Rubber Institute, London, 1985, p. 5.1.
- (2) J. A. Sauer, C. C. Chen; Polymer Eng. Sci.; Vol. 24,n.10,1984, pp.786-797.
- (3) Der-jin Woan, M. Habibullah, J. A. Sauer; Polymer, Vol.22, 1981, pp. 699-701.
- (4) J. L. Turkanis, R. W. Hertzberg, J. A. Manson; Deformation Yield and Fracture of Polymers, Plastics and Rubber Institute, Cambridge, 1985, p.54.1.
- (5) M. T. Hahn et al.; Deformation Yield and Fracture of Polymers, Plastics and Rubber Institute, Cambridge, 1982, p.19.1.
- (6) R. W. Hertzberg, J. A. Manson; "Fatigue in Engineering Plastics", Academic Press, New York, 1980.

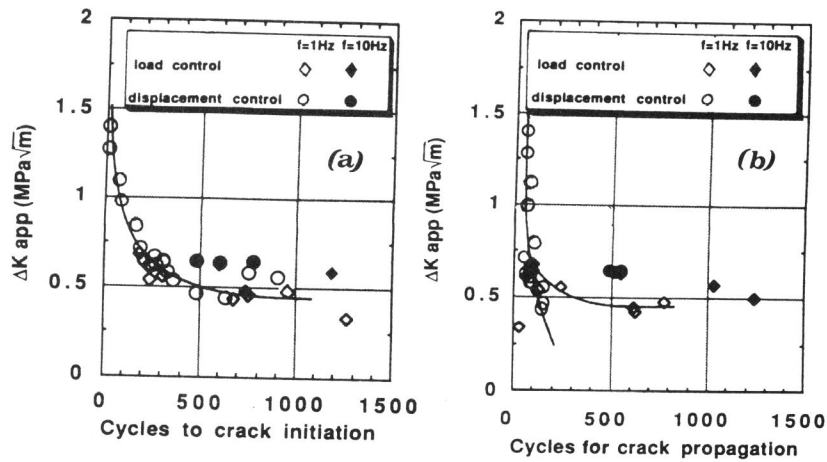


Figure 1. Number of cycles (a) to crack initiation, and (b) for crack propagation in sample AES-B27 in respect of a range of applied  $\Delta K$ .

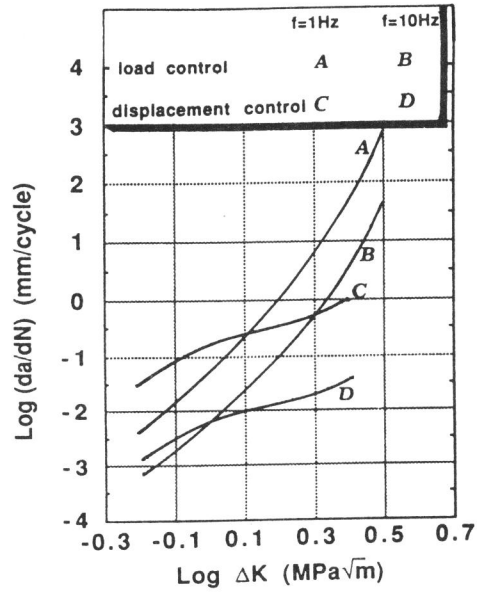


Figure 2. Fatigue crack growth data for sample AES-B27. Lines are averages of numerous tests.

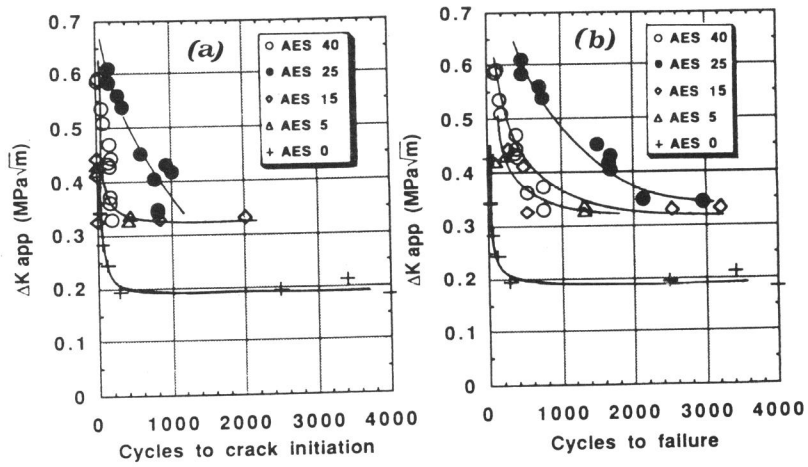


Figure 3. Effect of rubber content on number of cycles (a) to crack initiation, and (b) to failure for a range of applied  $\Delta K$ .